ICANS XIX,
19th meeting of International Collaboration on Advanced Neutron Sources
March 8 – 12, 2010
Grindelwald, Switzerland

Development of Fermi chopper at KEK

S. Itoh, K. Ueno, T. Yokoo, Y. Funahashi, T. Kamiyama[*], H. Sato[*], N. Miyamoto[*], Y. Kiyanagi[*], T. J. Sato[**], T. Otomo and S. Satoh
High Energy Accelerator Research Organization, Tsukuba, 305-0801, Japan,
[*]Hokkaido University, Sapporo, 060-8628, Japan,
[**]The University of Tokyo, Tokai, 319-1106, Japan

ABSTRACT

We developed a Fermi chopper by using a rotation system similar to a turbo molecular pump with a magnetic bearing. The control performance of the prototype as well as the transmission properties of candidate slit materials were investigated. Finally, the first model was completed.

1. Introduction

A Fermi chopper is a device to monochromatize a pulsed neutron beam [1]. It has a rotating slit package, and the rotational phase is synchronized to the repetition of the accelerator. At ISIS, the Fermi choppers rotating up to 600 Hz of the rotational frequency (f) have been in a practical use for a long time [2], and many chopper spectrometers have been constructed and maintained. We are constructing the High Resolution Chopper Spectrometer (HRC) at J-PARC [3-6], and the Fermi chopper is a key device to realize the resolutions of HRC. When we started a collaboration project at KEK between Neutron Science Division (KENS) and Mechanical Engineering Center (MEC) for the development of the Fermi chopper, there were no production results in Japanese venders. We have an experience of introducing foreign products, but a quick correspondence to an improvement plan of spectrometers cannot be easily expected. Recently, each pulsed neutron facility shows the tendency to secure the Fermi chopper individually. Therefore the domestic production has an important meaning on the security of the getting route.

To realize high resolution experiments using relatively high energy neutrons with a reasonable neutron flux on HRC, thinner slit materials for the slit package as well as higher rotational frequencies are indispensable [5]. Since the pulse width is Δt_m = 2.5 μs for the incident neutron energy E_i = 1 eV on HRC, the chopper opening time is required to be Δt_{ch} = 1.0 μs to obtain the energy resolution of $\Delta E/E_i$ = 1% [3]. To realize Δt_{ch} = 1.0 μs with f = 600 Hz, the slit width of w = 0.4 mm is required for the diameter (D = 100 mm) of the rotor inserting the slit package ($\Delta t_{ch} = w/2\pi Df$). But, the collimation of w/D = 4 mrad smaller than the incident beam divergence on HRC (5 mrad) reduces the neutron flux transmitted through the Fermi chopper. Since the thickness of the conventional slit material is approximately w' = 0.5 mm, the transmission is reduced to w/(w+w'). If thinner slit materials as well as higher rotational frequencies are realized, the transmission is improved. However, we started the development to realize the Fermi chopper rotating at 600 Hz first, to arrive at the world standard. It is noted that the phase control accuracy $\Delta t \leq$ 0.3 μs less than 30 % of Δt_{ch} is required to maintain the transmission [7].

2. Prototype

It was not easy for us to develop the magnetic bearing system, so we tried to realize the Fermi chopper by modification of a turbo molecular pump (TMP) with a magnetic bearing. We chose a TMP with 1300 L/s, because the mass and the moment of inertia of its rotor blade were almost identical to those of the rotor of the Fermi chopper. We confirmed that the rotational fluctuations (full width at half maximum) of this TMP were 0.099 μs, 0.205 μs, 0.221 μs and 1.998 μs at 600 Hz, 500 Hz, 300 Hz and 100 Hz, respectively, and the data at f = 600 Hz are shown in Fig. 1. This result is satisfied with the requirement of the phase control accuracy. Furthermore, since the maximum unbalance was reported to be 5 gmm on this TMP, we tried to operate this TMP adding an unbalance weight on the rotor blade, and confirmed a stable rotation within this range of unbalance. These results indicate the possibility of realization of the Fermi chopper by using this TMP. We produced a prototype of the Fermi chopper by replacing the blade of this TMP with the rotor with a slit package as shown in Fig. 2, where the outer diameter of the rotor was 125 mm and the length of the slit package was D = 98 mm.

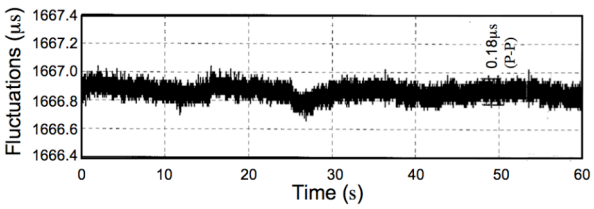

Fig. 1 The observed rotational fluctuations of the period on the TMP with 1300 L/s having the rotor blade rotating at 600 Hz as a function of the time. The width of 0.18 μs (p-p) is equivalent to 0.099 μs (FWHM).

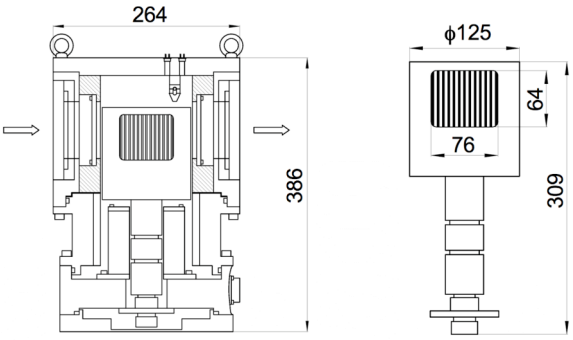

Fig. 2 The schematic drawing of the Fermi chopper produced by the modification of the TMP: an assembly (left) and a rotor (right).

First, we mounted a cylindrical rotor made of Al without a hole inserting the slit package and confirmed no resonance frequency up to 600 Hz. A minimum proper vibrational frequency was measured to be 1513 Hz by a hammering test, and this result was consistent with the stable rotation up to 600 Hz. Next, a slit package was inserted to the Al rotor. The slit package had the same structure as that used at ISIS [8]: the Al spacer had the same structure, but we used boron/epoxy composites for the slit materials described below. Since a deformation of the rotor prevents a stable rotation, we carried out calculations of stress distribution by the finite element method (FEM), to find the rotor shape and the material for minimizing the deformation at f = 600 Hz. If we chose A5056 as the rotor material, the largest displacement was calculated to be 3.4 mm and we estimated an unbalance at 600 Hz. The largest displacement was reduced to be 0.4 mm for ANB79, as shown in Fig. 3.

Based on this analysis, we designed the rotor of ANB79 inserting the slit package and produced the Fermi chopper shown in Fig. 2. We performed rotation tests with connecting the TMP controller delivered commercially to this Fermi chopper in the frequency range of f = 100 - 600 Hz. The axis displacement displayed on the TMP controller is plotted as a function of f in Fig. 4. The axis displacement was always below the trigger level for the emergency stop defined on the TMP controller up to 600 Hz.

We tried to investigate the possibility of f = 1 kHz in the design. In a preliminary analysis for the stress distribution, we found that the rotation at f = 1 kHz can be realized

by the size reduction of the rotor to 60 % of that of the solution for f = 600 Hz, i.e. D = 60 mm for f = 1 kHz. The product of Df was unchanged. This indicates that only an increase of f cannot reduce the chopper opening time $\Delta t_{ch} = w/2\pi Df$. However, since the collimation w/D can become larger, the neutron flux transmitted through the Fermi chopper can be increased. Further investigations are required for finding a structure for f = 1 kHz.

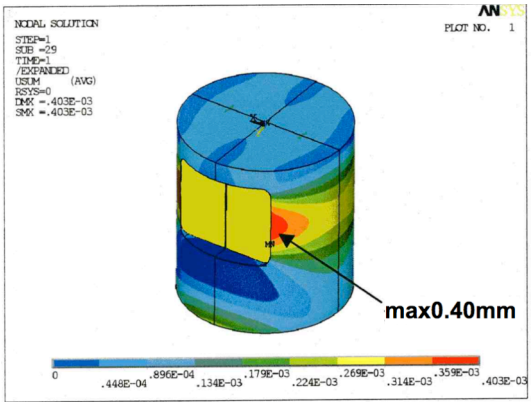

Fig.3 The calculation of the displacement in the rotor rotating at 600 Hz.

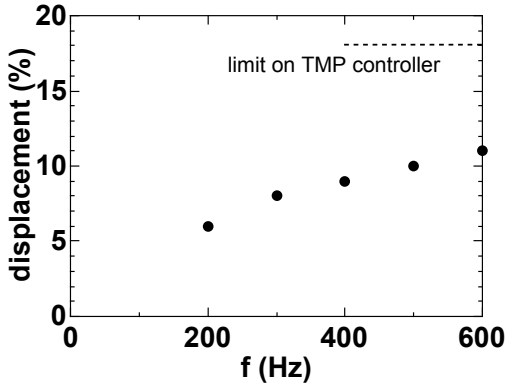

Fig. 4 The axis displacement as a function of the rotational frequency in the prototype of the Fermi chopper.

3. Control performance and actual model

First, we tried to design the phase control system of the Fermi chopper synchronized with the repetition of the accelerator by using the TMP controller delivered commercially, as shown in Fig. 5 (a). The TMP controller has an analog input terminal, and the rotational frequency can be controlled in the range of 100 - 600 Hz by applying the voltage of 0 - 5 V to the terminal, respectively. However, we found that the frequency can be changed by 1 Hz step (the frequency resolution of this system was $\Delta f = 1$ Hz). This resolution was not satisfied with the phase control accuracy. Since the relation between the frequency (f) and the period (t) is $f = 1/t$, the frequency resolution is described in the term of the timing accuracy as $\Delta f = |\partial f/\partial t|\Delta t = f^2\Delta t$. We require $\Delta t \leq 0.3$ μs for $E_i = 1$ eV, i.e. $\Delta f \leq 0.01$ Hz. In addition, the response time from the setting of the voltage to change the frequency was several seconds. This was also too large in comparison with Δt.

Next, we investigated the system where the TMP controller was used only for the magnetic bearing control and the motor was driven by an external inverter, as shown in Fig. 5 (b) (but the feedback circuit was removed). In the first trial, the system was rotated only up to 100 Hz, and then, broken at higher frequencies. After some trials, the acceleration rate of the frequency was measured for the system in Fig. 5 (a), and then the frequency was increased with the same acceleration rate in the system in Fig. 5 (b). However, the system showed an unbalance at 476 Hz and was not able to increase the frequency. Finally, by tuning the parameters of the magnetic bearing electrically, we successfully rotated this Fermi chopper system at 600 Hz by the external inverter in the system in Fig. 5 (b). Figure 6 shows the response property of this system without the feedback circuit. The observed frequency was 599.4 Hz ± 0.01 Hz for the setting of the frequency to 600.0 Hz by the inverter. By changing the setting value to 600.1 Hz or 599.9 Hz, the observed frequency was changed by the 0.1 Hz step, and similar rotational fluctuations were observed. This indicates that the system shown in Fig. 5 (b) has resolutions enough for the realization of the phase control accuracy.

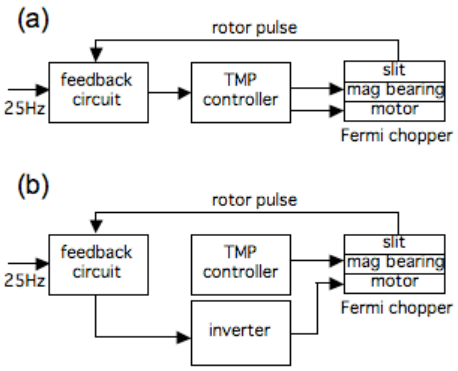

Fig. 5 Concept of the phase control: (a) by the TMP controller, (b) by the external inverter, where the TMP controller controls the magnetic bearing only.

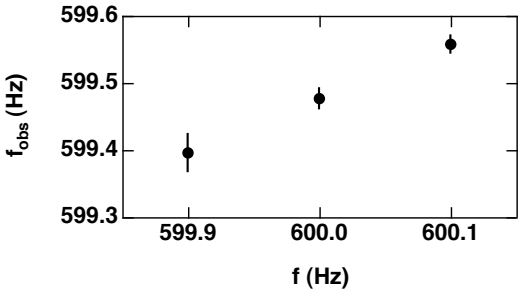

Fig. 6 The response property of this system without the feedback circuit in Fig. 5 (b). The observed rotational frequency for the frequency requested by the external inverter is plotted. The vertical bars represent the rotational fluctuations.

4. Slit materials

The slit package of the Fermi chopper used at ISIS consists of alternative layers of the boron/Al composites and the Al grids (Al spacers with a grid shape) [8]. A boron/Al composite is an array of boron fibers with the tensile stress of 36 GPa combined into Al plate by diffusion bonding, and the tensile stress of the composite is reported to be more than 500 MPa. Boron fibers are made of a tungsten core wire coated with boron by a chemical vapor deposition.

We tried to develop the boron/Al composite by using commercially available boron fibers (the outer diameter of 0.1mm). First, we tried to fabricate a small piece of the composite with the tensile strength more than 500 MPa. The drum of 200 mm diameter was wrapped with a stainless steel foil of 0.1 mm thickness, then a boron fiber was rolled with keeping the distance of 0.05 mm between the fibers on the foil. The fine particles of A6061 alloy with the size of 20 – 53 μm were sprayed on to the fibers eight times by the thermal spraying process and a preformed sheet was fabricated. Three preformed sheets were layered so that the fiber directions are perpendicular to those of the neighboring layers and an A6061 foil of 0.1mm thickness was on the top and the bottom. These components were combined by a diffusion bonding process under the conditions of 525 °C, 1 hour and 20 MPa in the vacuum hot press. Finally, a small composite of 20 mm × 20 mm was obtained. Figure 7 (left) shows the cross sectional picture of the piece. The tensile strength along the two-fiber direction of this piece was measured to be 600 MPa, as shown in Fig. 7 (right). It is noted that the averaged tensile strength along the two-fiber direction weighted by the volume fractions of the boron fiber and the Al matrix (the tensile stress of A6061: 152 MPa) was calculated to be 858 MPa on the assumption of no effect of the fibers perpendicular to the applied load. Next, in order to obtain a larger size of the composite for the actual use, the structure and the fabrication process were simplified. The array of boron fibers was sandwiched by pure Al foils of A1N30 as shown in Fig. 8 (left), then the single layer composite was fabricated by a diffusion bonding under 580 °C, 8 hours and 20 MPa in the vacuum. Figure 8 (middle) shows the cross sectional picture of the composite plate, and the thickness of the samples were in the range of 0.27 – 0.28 mm. Finally, pieces of the size of 65 mm × 98 mm of the composite were obtained. The array of boron fibers in this composite was not uniform, as shown in the X-ray transmission image in Fig. 8 (right), and the tensile strength was measured to be 220 MPa along the fiber direction smaller than the averaged tensile strength of 626 MPa.

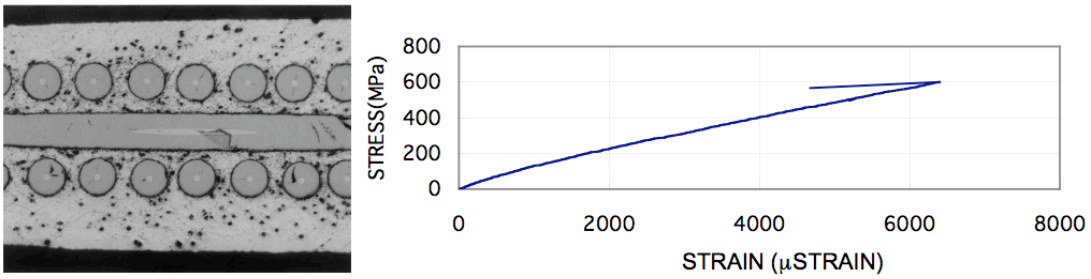

Fig. 7 The triple fiber layered slit material fabricated in our development: the scanning electron microscopy image of the cross sectional picture (left) and the stress-strain curve obtained by the tensile test (right).

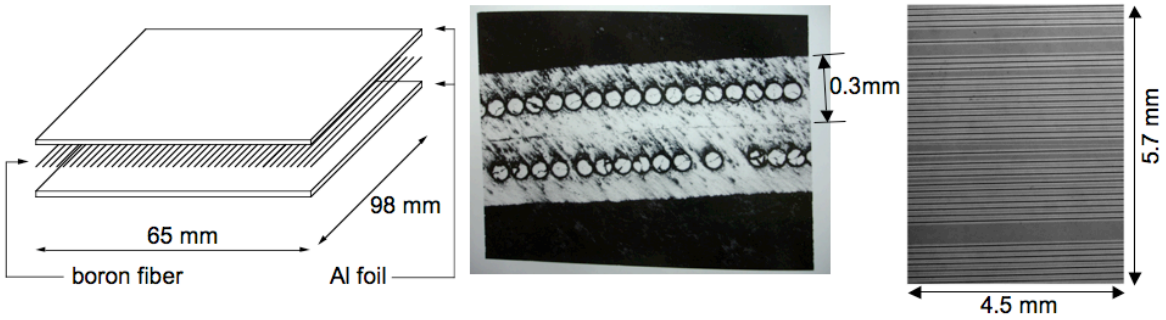

Fig. 8 The single fiber layered slit material: the structure of the composite (left), the scanning electron microscopy image of the cross sectional picture (middle) and the X-ray transmission image (right).

The other candidates for the slit materials were surveyed. One candidate material is a boron/epoxy composite which is commercially available. In this material, boron fibers are combined with a tough and rigid epoxy resin, and consist of three layers of the boron fiber array. The tensile strength is reported to be 1590 MPa. Another candidate material is a B_4C film, where B_4C powders are coated on both sides of a polyester film by using an adhesive agent. Two types of films are available: 12.5 μm B_4C + 25 μm polyester + 12.5 μm B_4C (total thickness is 50 μm) and 25 μm B_4C + 50 μm polyester + 25 μm B_4C (total thickness is 100 μm). We performed tensile tests for the B_4C films, as shown in Fig. 9.

We investigated the shielding performance of these slit materials by using a pulsed neutron source at the 45 MeV electron linear accelerator at Hokkaido University. The flat slit package consisting of the slit materials and the Al grids was mounted on a turntable at the distance of 12.38 m from the neutron source of which width was 0.1 m. The B_4C slit was mounted just at the upstream side of the slit package. The time-of-flight (TOF) spectrum as well as the spatial distribution of the transmitted neutrons through the slit package was measured with a two-dimensional position sensitive scintillator (PMRT) as a function of the angle between the slit package and the beam line. The experimental set-up is shown in Fig. 10. A typical spacial distribution and TOF spectrum of the neutrons transmitted through the slit package are plotted in Fig. 11. The intensity integrated over the TOF range of 0 – 20 ms in the TOF spectrum was plotted as a function of the angle in Fig. 12. The samples investigated here are listed in Table 1. The samples A, B and C are the single fiber layered boron / Al composites, where the fibers of 0.1 mm diameter arrayed with the pitch of 0.15 mm in the layer and the angle between the fiber and the neutron beam was chosen to be 0°, 5° and 10°, respectively. D is the single fiber layered boron / Al composite with the same fiber pitch as the diameter (0.1 mm) and with one fiber direction parallel to the beam. E is the triple fiber layered boron / epoxy composite available commercially with one fiber direction parallel to the beam. F and G are the B_4C foils with the total thickness of 50 μm and 100 μm, respectively. H is the double fiber layered boron / Al composite used at ISIS with one fiber direction parallel to the beam.

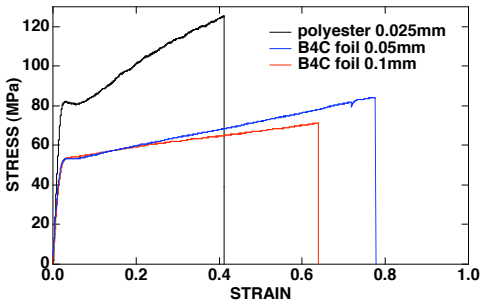

Fig. 9 Stress-strain curves normalized by the sample thickness of B_4C foils and polyester.

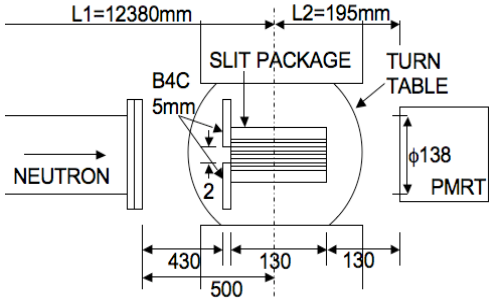

Fig. 10 Experimental set-up to measure shielding performance of the slit materials.

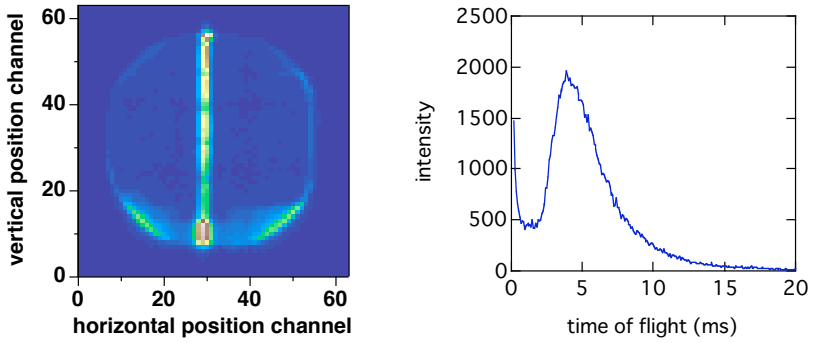

Fig. 11 A typical special distribution of the intensity detected at the PMRT (left) and the TOF spectrum of the neutrons transmitted only through the slit package (right).

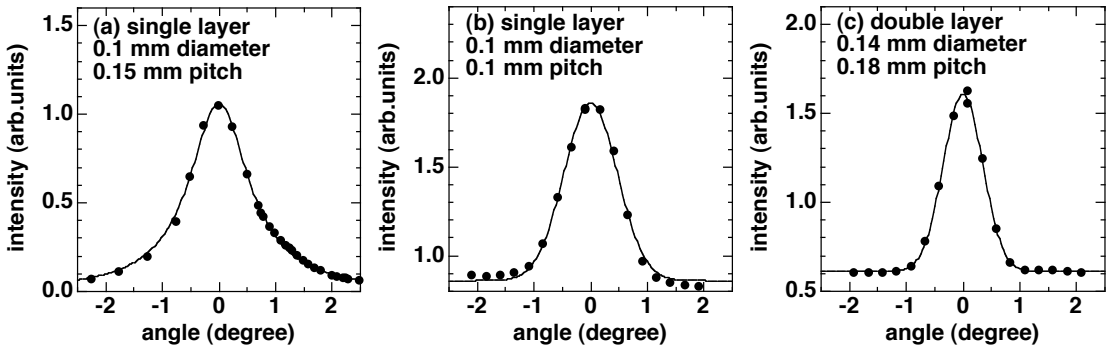

Fig.12 The angular dependence of the transmitted intensity through the slit package sample: (a) A, (b) D, (c) H. The solid lines are the fitted Lorentzian (a) and Gaussian ((b),(c)) curves. The constant background intensity is the high energy neutrons transmitted through the sample system.

Table I Shielding performance of various slit materials. w' is the thickness of the sample material, Δθ is the observed half width of the angular dependence in Fig. 12, w_{eff} is the effective slit spacing obtained from Δθ.

sample	structure	w' (mm)	Δθ(°)	w (mm)
A	Boron(0.1mm)/Al, single layer, pitch=0.15mm, 0°	0.3	(Lorentzian)	-
B	Boron(0.1mm)/Al, single layer, pitch=0.15mm, 5°	0.3	0.582	1.725
C	Boron(0.1mm)/Al, single layer, pitch=0.15mm, 10°	0.3	0.622	1.721
D	Boron(0.1mm)/Al, single layer, pitch=0.1mm, 0°	0.3	0.556	1.732
E	Boron(0.1mm)/epoxy, triple layer	0.5	0.459	1.359
F	B_4C film (12.5+25+12.5=50μm)	0.05	0.416	1.187
G	B_4C film (25+50+25=100μm)	0.1	0.421	1.208
H	Boron(0.14mm)/Al, doube layer (ISIS/KENS)	0.5	0.410	1.162

The angular dependence of the transmitted intensity through the sample A was fitted with a Lorentzian. This indicates that neutrons were leaked through the vacancy showed in Fig. 8 (right). The angular dependences for the other samples were well fitted with a Gaussian, and the half width at the half maximum, $\Delta\theta$, for each curve was determined. The observed half width can be described by $\Delta\theta = [(w_{eff}/L_{slit})^2+(\Delta\phi_i)^2]^{1/2}/2$, where w_{eff} is the effective slit spacing, L_{slit} is the length of the slits and $\Delta\phi_i = 8$ mrad is the incident beam divergence. $L_{slit} = 92.4$ mm for B and $L_{slit} = 85.3$ mm for C, and $L_{slit} = 98$ mm for the other samples. We obtained w_{eff} from $\Delta\theta$, as listed in Table I. If the absorption cross section of the slit materials is large enough, w_{eff} equals to the spacing between the slit materials, 1.2 mm. Within this analysis where low energy neutrons are dominant, F and G have a good shielding performance. However, we found the deformation of the slit materials F in the rotor of the Fermi chopper rotating at 600 Hz. Therefore, H is still the best slit material in the present investigations. Further investigations are required to find thinner slit materials with good shielding performance.

5. Actual model production and summary

Based on the developments, we produced the first model of the Fermi chopper made in Japan, as shown in Fig. 13. A magnetic bearing system similar to that for the TMP was used. The commercially available materials, boron fiber/epoxy composites, were used for the slit materials. The lowest proper vibrational mode was measured to be at 800 Hz larger than the maximum operational frequency of 600 Hz. Normally, electrical noises occur in an inverter system. In the actual model, by replacing the inverter by a direct digital synthesizer (DDS), electrical noises were successfully reduced; also much better control accuracy of 0.01 Hz was achieved. A shifting mechanism of two Fermi choppers was also developed, as shown in Fig. 13. In this actual system, we confirmed the phase control accuracy less than 0.3 μs at 600 Hz against the timing of the external trigger. The investigations of the slit materials are still in progress.

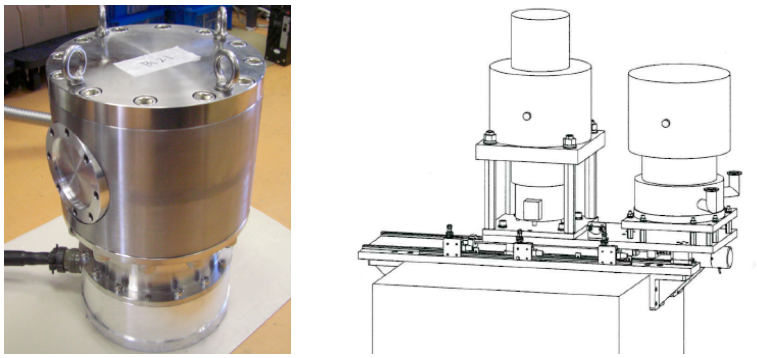

Fig. 13 The first Fermi chopper made in Japan (left) and its shifting mechanism for two choppers (right).

References

[1] E. Fermi et al., Phys. Rev. 72 (1947) 193.
[2] T. J. L. Jones et al., Proceedings of ICANS-VIII (1985) 707.
[3] S. Itoh et al., J. Neutron Research 13 (2005) 59.
[4] S. Itoh et al., Proceedings of ICANS-XVII (2006) 1019.
[5] S. Itoh et al., Proceedings of ICANS-XVIII (2007) 362.
[6] S. Itoh at al., Proceedings of ICANS-XIX (2010) this issue.
[7] S. Itoh, Proceedings of ICANS-XV (2001) 327.
[8] T. J. L. Jones, "Fermi chopper slit packages for 1eV neutrons", unpublished.